# Chapter 7

# Lift and drag: Paradoxes of nonviscous flow

At large  $\mathcal{R}$  the flow past an object can often be described by the Euler equation or even as a potential flow. We will show that the *lift* acting on an airplane wing, as well as part of its drag, can be described by the nonviscous theory, provided that viscous effects in the boundary layer are made allowances for in a nontrivial way. Eventually we will se what this theory predicts for the lift on rotating bodies.

### 7.1Forces on bodies in a flowing fluid

The everyday observation that an airplane may stay in the air provided there is still fuel left, is related to the lift and the drag acting on it, perpendicular to and against the direction of motion, respectively. The triviality of this becomes less evident once we try to predict the forces from basic fluid dynamical principles—if the air had been an ideal fluid, air travel as we know it would not have been possible.

Consider a body at rest in a stationary incompressible fluid flow in the x direction, as drawn in Figure 7.1, where the body is assumed to be a part of an airplane wing with a constant chord c. We will assume  $\mathcal{R} \gg 1$  and  $\mathcal{M} \ll 1$  as well as a uniform flow at large distances from the body, thus the incoming flow is irrotational:

$$\boldsymbol{u} = \boldsymbol{u}_0 + \boldsymbol{u}' \tag{7.1}$$

$$u = u_0 + u'$$

$$\lim_{r \to \infty} u' = 0$$

$$p = p_0 + p'$$

$$\lim_{r \to \infty} p' = 0$$

$$(7.1)$$

$$(7.2)$$

$$(7.3)$$

$$p = p_0 + p' \tag{7.3}$$

$$\lim_{r \to \infty} p' = 0 \tag{7.4}$$

For brevity we will not include effects of gravity. The body is enclosed in a fixed control volume whose total surface S is permeable to the flow. If F is the force from the fluid on the body, then by the impulse-momentum principle (??)/(??) its reaction force equals the total momentum flow rate through the control volume:

$$-\mathbf{F} = \oint_{S} \Pi_{ik} \hat{\mathbf{e}}_{i} \hat{n}_{k} \, dS \tag{7.5}$$

$$\Pi_{ik} = (p_0 + p')\delta_{ik} + \rho(u_{0i} + u'_i)(u_{0k} + u'_k)$$
(7.6)

Figure 7.1: A control volume containing a body

Irrespective of the form of the control volume's surface, the following relations hold:

$$\oint_{S} d\mathbf{S} = 0 \tag{7.7}$$

$$\oint_{S} d\mathbf{S} = 0$$

$$\oint_{S} \rho u_{0i} u'_{k} \hat{n}_{k} dS = \rho u_{0i} \oint_{S} \mathbf{u}' \cdot d\mathbf{S}$$

$$= 0 \quad \text{(inkompressibel fluid)}$$
(7.7)

Thus,  $\Pi_{ik}$  in the integral for the total momentum flow rate can be simplified:

$$\Pi_{ik} \stackrel{eff}{\to} p' \delta_{ik} + \rho u_{0k} u_i' + \rho u_i' u_k' \tag{7.9}$$

As in Figure 7.1 we let the control volume be limited by two planes perpendicular to the xaxis, at  $x_2$  in front of the wing and  $x_1$  behind it, respectively. We place its limitations in the y and z directions out at infinite distance, where the contributions to the integral (7.5) from these parts of the surface become zero, since the deviations from an uniform flow disappear there.1

By moving  $x_2$  far enough from the wing, evidently the conditions for potential flow will be satisfied there; viscous effects can only be of importance in the boundary layer at the wing, and without viscous effects present there will be a zero circulation according to the Kelvin-Helmholz theorem. From Bernoulli's theorem on the form (??), and from the condition that

<sup>&</sup>lt;sup>1</sup>Several textbooks make an elegant jump over the reason that this is allowed: For  $\mathcal{R}\gg 1$  and an irrotational incoming flow, we have potential flow at large distances from the wing. The centrally symmetric part of the most slowly decreasing solution to Eq.  $\nabla^2 \Phi = 0$  goes as 1/r for large r (it is sufficient to consider this part since the angular contributions will decrease as fast), see for instance Eq. (??). u', and thus according to Bernoulli's likning (??) also p', will then decrease as  $1/r^2$  or faster. Since the total area of the sides parallel to the x axis will increase proportional to r for fixed  $x_1$  and  $x_2$ , the contribution to the integral on these sides will approach zero.

the potential must approach a constant in the limit  $\sqrt{y^2+z^2}\to\infty$ , respectively, we then get

$$p' + p_0 + \frac{1}{2}\rho(\mathbf{u}_0 + \mathbf{u}')^2 = p_0 + \frac{1}{2}\rho u_0^2$$

$$(x = x_2)$$

$$p' + \rho u_0 u_x' + \rho u_x'^2 = \frac{1}{2}\rho(u_x'^2 - u_y'^2 - u_z'^2)$$
(7.10)

where  $u_0 = u_{0x} = |u_0|$ , and

$$\iint_{(x=x_2)} u'_y \, dy \, dz = - \iint_{(x=x_2)} \frac{\partial \Phi}{\partial y} \, dy \, dz = 0$$
 (7.11)

$$\int \int_{(x=x_2)} u_z' dz dy = - \int \int_{(x=x_2)} \frac{\partial \Phi}{\partial z} dz dy = 0$$

$$(7.12)$$

The contributions to  $F_y$  and  $F_z$  from the plane at  $x = x_2$  will then be zero. The calculation of the contribution to  $F_x$  at this plane reduces to an integral over the second powers of the deviations from uniform velocity; as already mentioned in a footnote these components decrease sufficiently fast for increasing distance that neither  $F_x$  receives any contribution at this plane when it is moved far in front of the wing.

The calculation of the force components has been reduced to integrals over the plane behind the wing:

$$F_x = - \int \int_{(x=x_1)} (p' + \rho u_0 u_x' + \rho u_x'^2) \, dy \, dz$$
 (7.13)

$$F_y = - \int \int \int (\rho u_0 u'_y + \rho u'_x u'_y) \, dy \, dz$$
 (7.14)

$$F_z = - \int \int_{(x=x_1)} (\rho u_0 u_z' + \rho u_x' u_z') \, dy \, dz$$
 (7.15)

In this calculation we can no longer argue for a pure potential flow even for  $x_1$  far from the body. As indicated in connection with Figure 3.2, there will be a wake in the flow behind the body. The part of the fluid which passed by the body along streamlines in the boundary layer or close to it, where viscous effects give important contributions, will flow through the  $x_1$  plane. The wake is called laminar or turbulent depending on whether the flow in the boundary layer is laminar or turbulent.<sup>2</sup>

In later chapters we will give a qualitative description of some wake types.<sup>3</sup> In what follows here, what matters to us is that the integration plane's intersection with the wake will occupy a decreasing fraction of the total solid angle around the body the further away  $z_1$  is, see Problem 7.2.

<sup>&</sup>lt;sup>2</sup>At large distances behind the wing a turbulent wake will become laminar.

<sup>&</sup>lt;sup>3</sup>A laminar wake behind a streamlined thin body can be described quantitatively by a corresponding formalism as in the next chapter, where laminar boundary layers are treated.

Figure 7.2: Nonviscous flow: Streamline symmetry at a symmetric body

## 7.1.1 d'Alembert's paradox

Suppose for a moment that the flow is purely nonviscous everywhere, and accordingly completely irrotational. Then we will have potential flow everywhere, and the integrand in Eq. (7.13) can be replaced as in Eq. (7.10). According to the same type of argument as above, the integral will then approach zero. This is one of several equivalent ways of deducing  $d'Alembert's\ paradox$ :

• A stationary flow of an ideal fluid past a body at rest will give no drag force on the body

We saw some explicit examples of this in Problems 3.1 and 3.2, where the geometrical symmetry resulted in a symmetric pressure distribution. For a more general upstream/downstream symmetry as in Figure 7.2, we have an analogous situation: If  $\Phi$  is a solution of Eq. (??), then also  $-\Phi$  will be a solution; the streamline and pressure patterns will be the same in the two cases, only with the velocity arrows inverted. The upstream/downstream symmetry will then give a full symmetry in the pressure patterns, and the drag force will trivially become zero.

One may argue that it would have been a greater paradox if a completely nonviscous theory had given rise to a drag force. Suppose that a body is pulled with a constant velocity through such a fluid. An eventual drag force would the do a work on the fluid. However, in the absence of viscous dissipation the kinetic energy of the fluid would have to be continuously increasing, and no stationary state would be possible.

### 7.1.2 Kutta-Joukowski's theorem

We will now see what the cottesponding nonviscous theory predicts for the lift, i.e., the force component perpendicular to the fluid flow direction, with the approximation two-dimensional flow in the xz plane. Let L be the total wing span, and make the extra assumptions

- $L \gg c$  (large aspect ratio)
- Thin wake, 4 irrotational flow outside of it

<sup>&</sup>lt;sup>4</sup>See Problem 7.2 for the justification.

Figure 7.3: Integration path for 2D calculation of lift

Furthermore, let  $x_1$  have a fixed finite value. The integration in Eq. (7.15) passes through the wake, where the potential theory is invalid, since the viscosity may create vorticity there. Since  $u_0 \gg |u_x|$ , and  $|u_z|$ 's value is not of a different order of magnitude inside of the wake compared to outside, we can convert Eq. (7.15) as follows:

$$F_{z} = -\rho u_{0} \int \int u_{z} dy dz$$

$$\approx -\rho u_{0} L \int_{-\infty}^{\infty} u_{z} dz$$

$$\approx \rho u_{0} L \left( \int_{-\infty}^{z_{2}} \frac{\partial \Phi}{\partial z} dz + \int_{z_{1}}^{\infty} \frac{\partial \Phi}{\partial z} dz \right)$$

$$= \rho u_{0} L \left( \Phi_{2} - \Phi_{1} \right)$$

$$(7.16)$$

The indices 1 and 2 for z and  $\Phi$  refer to the upper and lower border of the wake, respectively. However, we can also express the potential difference by an integral over a finite path in the irrotational part of the flow, as in Figure 7.3. The assumption about a thin wake can then be used to extend the integration path into a closed loop passing through the wake:

$$\Phi_{2} - \Phi_{1} = \int_{C} \operatorname{grad} \Phi \cdot d\boldsymbol{l}$$

$$= -\int_{C} \boldsymbol{u} \cdot d\boldsymbol{l}$$

$$\approx -\Gamma \tag{7.17}$$

With

$$\mathcal{L} = \frac{F_z}{L} \tag{7.18}$$

we have thus arrived at *Kutta-Joukowski's theorem*, which gives the lift per unit length of the wing expressed by the *circulation* around the wing:

$$\mathcal{L} = -\rho u_0 \Gamma \tag{7.19}$$

Figure 7.4: Lift due to pressure differences

The integration path can in principle be an arbitrary path around the wing outside the boundary layer. That there can be a nonzero circulation around the wing even in an irrotational incoming fluid is not a paradox in itself, since vorticity can be created in the boundary layer.

On the other hand, if one lets the wing start from zero velocity in an irrotational fluid and lets the integration path be so large that it comprises both the wing's start position and its later positions for a finite span of time, then seemingly the circulation around the loop changes with time. No trivial feat, since that would be a violation of Kelvin-Helmholz's circulation theorem!

## 7.1.3 Lift from Bernoulli's equation

Before turning in the next section to the dissolution of the abovementioned paradox, we will mention how the magnitude of the lift can be found in a simple way. If the curvature of the wing profile is such that the length of the upper side's cross-section curve is larger than that of the lower side's length, that may imply a larger flow velocity above the wing than below. According to Bernoulli's equation (??) the pressure will then be lowest on the upper side. In an iedal fluid the lift on the wing can only be due to the pressure difference between the lower and upper side, as indicated in Figure 7.4. The lift will then be directly related to the velocity difference via Bernoulli's equation.

In Problem 7.1 you will be asked to use this method, assuming there is potential flow everywhere outside the wing profile, to show that precisely the Kutta-Joukowski theorem will follow.

# 7.2 Viscous generation of circulation

When an irrotational fluid is set in motion past a wing which may provide lift, the flow pattern will be as in Figure 7.5a, with the rear stagnation point (separation point for streamlines in the boundary layer around the wing) on the upper side, at some distance from the rear edge. For an ideal fluid the pattern would be staying that way for as the speed increases, without circulation and without lift. However, viscosity in the boundary layer will make the separation point move to the rear edge (Figure 7.5b). A circulation around the wing has then become

Figure 7.5: Flow around wing profile, a) without and b) with circulation

Figure 7.6: The life story of a starting vortex. a) Cause, b) separation, c) transport towards its viscous death

established. This sudden move of the separation point will generate a *starting vortex* at the rear edge of the wing, with the same absolute value for its circulation as the wing's, only with the opposite direction. It will separate from the wing and follow the flow backwards, as shown in Figure 7.6. All this has been proved experimentally, as exemplified in Figure 7.7. Accordingly, Kelvin-Helmholz's theorem is still satisfied, provided the material loop is choosen large enough.

The complete three-dimensional truth, when we incorporate the wing's finite value of L/c, is somewhat more intricate. Let the integration path around the wing profile be locate in a surface constituting a 'mitten' on the wing tip, and outside the boundary layer, as in Figure 7.8. From Stokes's theorem (??):

$$\int_{S} \boldsymbol{\omega} \cdot d\boldsymbol{S} = \oint_{L} \boldsymbol{u} \cdot d\boldsymbol{L}$$

I.e., for a nonzero circulation there will be a net transport of vorticity out through the mitt surface due to the flowing fluid. The consistency of this follows from the fact that when there is lift present, the pressure will be greater below the wing than above, and outside the wing tip there will be a flow from the lower side to the upper side. Since this flow is superposed on the main perpendicular flow, there will be a wing tip vortex following the flow downstream from the wing, as shown in Figure 7.9. (Neither this is a violation of Kelvin-Helmholz's theorem, since a vortex with the opposite rotation direction will flow from the opposite wing

Figure 7.7: Photo of the separation of a starting vortex

tip.) Wing tip vortices from large aircraft can contain a considerable amount of circulation 10-20 km downstream, before they fade away.<sup>5</sup> The rotating 'steam jet' which air passengers may sometimes observe behind a wing tip in damp weather, is caused by condensation in the tip vortex due to pressure changes which follow from Bernoulli's law.

The circulation in the wing tip vortices is created *outside* the boundary layer. However, the presence of viscosity is still a requirement for a nonzero circulation around the wing profile, which in its turn is a prerequisite for the existence of wing tip vortices.

If a wing's angle of attack, the angle between the wing chord and  $u_0$ , becomes large enough, the separation point may move abruptly from the proile's rear end to a point near its front end, as shown in Figure 7.10, with strong subsequent fluctuations. A major part of the lift

Figure 7.8: Loop and surface for Stokes's theorem

<sup>&</sup>lt;sup>5</sup>It is not advisable for small planes to take off from a runway just behind a 'jumbojet' . . .



85

Figure 7.9: Starting vortex and wing tip vortices behind a plane

Figure 7.10: Stalled wing profile

will then disappear, a phenomenon called stalling.<sup>6</sup>

#### 7.2.1Induced drag

The wing tip vortices give rise to a component of the drag force which adds to the viscous drag in the boundary layer and the drag due to a viscous wake. Like the existence of wing tip vortices, this drag force would appear even in an ideal fluid. These vortices imply a downward component of the flow velocity in the fluid behind the wings. Thus, the effective flow past the wing will arrive slightly from above, decreasing the angle of attack. The lift force vector will be perpendicular to the effective direction of flow past the wing, which thus gets a component along  $u_0$ 's direction, called the *induced drag force*.

The effect can be minimalized by choosing as large an aspect ratio (= L/c) as possible. That is the reason why modern glider planes have very long and narrow wings.

It is no paradox that the effect would be present even in an ideal fluid. The work done by the induced drag force would not get lost, but would live on as rotational energy in the wing tip vortices.

#### 7.3Coefficients for lift and drag

By dimensional analysis one can express the lift and drag forces as

$$|F_z| = \frac{1}{2} C_L \rho u_0^2 Lc$$

$$|F_x| = \frac{1}{2} C_D \rho u_0^2 Lc$$
(7.20)

$$|F_x| = \frac{1}{2}C_D\rho u_0^2 Lc \tag{7.21}$$

where the dimensionless coefficients  $C_L$  and  $C_D$  are functions of the dimensionless parameters in the flow problem.<sup>7</sup> Assume now:

- Negligible effects due to surface tension and gravity waves
- $\mathcal{M} \ll 1$ , incompressible fluid, valid potential flow description (approximately instantaneous propagation of pressure changes)

Then the coefficients of a given profile can be expected to be functions of the angle of attack and the Reynolds number only:

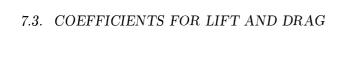
$$C_L = C_L(\alpha, \mathcal{R}) \tag{7.22}$$

$$C_D = C_D(\alpha, \mathcal{R}) \tag{7.23}$$

The magnitude of the C's will also depend on the wing profile and its assymmetry, with schematic examples shown in Figure 7.11. An effective wing ought to have  $C_D \ll C_L$ , which is obtained for streamlined and thin profiles. Figure 7.12 shows an example of coefficients for a standard wing profile at a given large Reynolds number, based on chord length. The stalling phenomenon appears clearly, with boundary layer separation / decrease of lift as well as drag increase, for angles of attack larger than approximately 12°.

<sup>&</sup>lt;sup>6</sup>Aircraft are constructed such that the tail plane will normally operate under conditions farther from stall than the wings. Some degree of control is then present even when one or both wings stall.

 $<sup>^{7}</sup>Lc$  is the planform area. The use of it instead of  $L^{2}$  is a departure from a 'pure' dimensional analysis. Another example of such a departure is that  $C_D$  in Eq. (??) is sometimes defined with  $\pi D^2/4$  explicitly in the equation, instead of  $D^2$ .



87

Figure 7.11: Examples of wing profiles, with chord and angle of attack indicated

Figure 7.12: Coefficients for the profile RAF 34 for  $\mathcal{R}=4.5\cdot 10^6$ . The ideal relation  $C_L=2\pi\alpha$  drawn with a broken line

An exact theoretical result for  $C_L$  is known for the case of a flat and thin profile with infinite aspect ratio, in the limit of small angles of attack, where the circulation and thus the lift can be calculated [Landau and Lifshitz 1987]:

$$C_L = 2\pi\alpha \tag{7.24}$$

A theoretical minimum value of the coefficient  $C_{D,ind}$  for induced drag can also be derived:<sup>8</sup>

$$(C_{D,ind})_{min} = \frac{c}{\pi L} C_L^2 \tag{7.25}$$

In Figure 7.12 the relation (7.24) has been drawn. We notice a good qualitative agreement with the experimental  $C_L$  values, which also depend approximately linearly on  $\alpha$  for small angles.

# 7.4 Lift on rotating bodies

A rotating body in a uniform fluid flow will be influenced by a force perpendicular to the flow direction in addition to the drag force. For a rotating cylinder or sphere<sup>9</sup> it is called the  $Magnus\ effect.^{10}$ 

Let us try to describe the Magnus effect quantitatively in the potential flow approximation, however now assuming a viscous interaction at the surface. The fluid close to it will be pulled in the direction of the rotation and gets its largest velocity on the side where the surface moves in the same direction as the fluid flow. Bernoulli's equation predicts the lowest pressure there, and thus a net force on the body towards that side, perpendicular to the flow.

For a cylinder this is simulated in Problem 7.4, with a line vortex superposed on a uniform potential flow past a non-rotating cylinder. This results in a description of an irrotational flow past a rotating cylinder, with a no-slip condition at its surface. The result for the 'lift' on the cylinder agrees with Kutta-Joukowski's theorem, and if the circulation is defined on the basis of the cylinder's surface rotation velocity by

$$\Gamma = 2\pi R u_s \qquad , \qquad u_s = (u_\phi)_{r=R} \tag{7.26}$$

then the lift coefficient follows from Eq. (7.19):

$$\frac{1}{2}C_{L}\rho u_{0}^{2}2R = \rho u_{0}2\pi R u_{s}$$

$$C_{L} = 2\pi \frac{u_{s}}{u_{0}} \tag{7.27}$$

We find qualitative agreement between practice and this theory for large rotation rates at least—the correct direction of the deflection force is predicted. Quantitative agreement is a different matter; even if the measured lift indeed does increase with the roughness of the cylinder surface, the theory predicts a values of  $C_L$  which is about a factor 2 too large. In this potential flow approximation,  $C_D$  can of course not be predicted at all.

<sup>&</sup>lt;sup>8</sup>The calculations, which may be accomplished using complex analysis, are comparatively simple. However, including them here would be beyond the scope of this course.

<sup>&</sup>lt;sup>9</sup>In the case of a sphere, the term *Robins effect* is sometimes used.

<sup>&</sup>lt;sup>10</sup>Which has wellknown applications (often unwanted) in soccer, baseball, tennis, golf and the firing of rifle shots!

7.5. PROBLEMS

Figure 7.13: Lift coefficient for a rotating sphere, as a function of  $u_s/u_0$ 

For low rotation rates the theory becomes still more dubious. Experimental results for a rotating sphere are shown in Figure 7.13, with the deflection pointing in the *opposite* direction for low rates.

The reason for this is that a cylinder or sphere is not a 'streamlined' body. Boundary layer separation will occur so early that a considerable part of the periphery is surrouded by turbulent flow (not potential flow). For low rotation rates we may have a transition from a laminar to a turbulent boundary layer on the side where the velocity difference between the flow and the surface is largest, before the boundary layer has become separated. By anticipating still more of the treatment of boundary layer separation (see a later chapter): A turbulent boundary layer delays the separation, and the general flow pattern will be as in Figure 7.14(a). This in contradiction to the pattern in 7.14(b) which is predicted by the theory presented above.

To learn more about the physics behind potential flow, evidently we have to study the boundary layer and the processes there in greater detail. That will be the theme of the subsequent chapters.

## 7.5 Problems

**Problem 7.1** Derive Kutta-Joukowski's formula in a simplified way: Assume a thin wing profile with a smooth flow with a constant velocity (although different values) along the upper and lower side, with separation precisely at the rear edge. Assume potential flow everywhere, and use Bernoulli's equation.

Figure 7.14: Flow pattern around a sphere for (a) asymmetrical boundary layer separation, and (b) as predicted for a conventional Magnus effect

**Problem 7.2** Use arguments about orders of magnitude as in Chapter 3 to determine the thickness a of the wake at a distance x behind a thin wing. Show that

- a)  $\frac{a}{x} \sim x^{-1/2}$  for a laminar wake
- b)  $\frac{a}{x} \sim x^{-2/3}$  for a turbulent wake

**Problem 7.3** An aircraft has mass  $10000 \,\mathrm{kg}$ , wing chord  $3 \,\mathrm{m}$  and total wing span  $30 \,\mathrm{m}$ . Find the magnitude of the circulation velocity around the wings, if the aircraft's velocity is  $360 \,\mathrm{km} \,\mathrm{hr}^{-1}$ .

**Problem 7.4** a) Show that the 2D velocity field

$$u_r = u_0 \left(1 - \frac{R^2}{r^2}\right) \cos \phi$$

$$u_\phi = -u_0 \left(1 + \frac{R^2}{r^2}\right) \sin \phi - \frac{\Gamma}{2\pi r}$$

is a solution for 2D *irrotational* flow past a circular cylinder with radius R, with uniform free flow velocity  $u_0$  in the positive x direction at large distance from the cylinder, and *circulation*  $\Gamma$  ( $\Gamma > 0$ ) in the negative direction of rotation around the cylinder.

b) Find the pressure distribution at the cylinder surface, and show that the lift per unit length of the cylinder is given by Kutta-Joukowski's theorem.